Synthesis of magnetic core-shell $Fe_3O_4@SiO_2@Mg(OH)_2$ composite using waste bischofite and its catalytic performance for ozonation of antibiotics

Jun Wu[a,b], Qi Sun[c], Jian Lu[c,*]

[a] Yantai Research Institute and Graduate School, Harbin Engineering University, Yantai, Shandong 265501, People's Republic of China
[b] College of Materials and Chemical Engineering, Harbin Engineering University, Harbin, Heilongjiang 150001, People's Republic of China
[c] CAS Key Laboratory of Coastal Environmental Processes and Ecological Remediation, Yantai Institute of Coastal Zone Research (YIC), Chinese Academy of Sciences (CAS), Shandong Key Laboratory of Coastal Environmental Processes, YICCAS, Yantai Shandong 264003, People's Republic of China

ARTICLE INFO

ABSTRACT

This study investigated the possibility of recycling bischofite which was discarded with a great quantity from salt industry as catalyst for ozonation of sulfathiazole. Bischofite was used to successfully synthesize nano-scaled magnetic core-shell $Fe_3O_4@SiO_2@Mg(OH)_2$ which could be easily separated for reuse by an external magnetic field. Element mapping showed that this composite microsphere was composed of a Fe_3O_4 core, a SiO_2 shell and a $Mg(OH)_2$ outer shell. Reaction rate, operation conditions, mineralization, and antibacterial activity of catalytic ozonation of sulfathiazole using $Fe_3O_4@SiO_2@Mg(OH)_2$ were investigated. The reaction rate constant of $Fe_3O_4@SiO_2@Mg(OH)_2$ treatment was almost twice that of single ozonation. Operation conditions including catalyst dosage of 0.15 g/L, pH of 7.0, and temperature of 25 °C were optimal for removal of sulfathiazole by catalytic ozonation. Over 99.0% of sulfathiazole could be removed within 10 min by catalytic ozonation with $Fe_3O_4@SiO_2@Mg(OH)_2$. About 99.0% of sulfathiazole could be removed by catalytic ozonation with $Fe_3O_4@SiO_2@Mg(OH)_2$ that was reused 4 times. About 40.1% of total organic carbon was removed within 60 min by catalytic ozonation with $Fe_3O_4@SiO_2@Mg(OH)_2$ to exhibit good mineralization feature for sulfathiazole. Catalytic ozonation played important role in affecting antibacterial activity of sulfathiazole. Initial concentration of sulfathiazole and inorganic ions had negative effect on removal efficiency. Sulfathiazole was degraded through cleavage and oxidation processes during catalytic ozonation by $Fe_3O_4@SiO_2@Mg(OH)_2$. This study provides a new core-shell magnetic material for antibiotic pollution control and a promising new application pathway for using waste bischofite.

1. Introduction

Bischofite is a mineral generally formed in the evaporation ponds of KCl production process [1] and it generally serves as the important by-product of salt industry. It has been reported that approximately 10 tons of bischofite is generated when 1 ton of KCl is produced [2]. However, only 8% of bischofite has been used in market [1] due to its limited applications to cause massive waste of magnesium resources. Although studies on usage of bischofite have been paid attention in recent years and bischofite has been used to prepare different functional materials [1–4], high-value utilization of bischofite is still a great challenge in terms of current application limitations of magnesium materials. It is urgent to investigate the possibility of recycling bischofite from salt industry.

Antibiotics, the greatest medical discovery in the 20th century, have been widely used for treating illness of humans and animals as well as

promoting growth of cultured animals [3–5]. Approximately 30%-90% of the consumed antibiotics by humans and animals are excreted by feces and urines [6]. The excreted antibiotics enter the environments through different pathways to pose the potential risks to the ecosystems and human beings [7,8]. Therefore, it is necessary to effectively control the release of antibiotics and efficiently remove these antibiotics.

Antibiotics have been detected in different aquatic environments with concentrations ranging from ng/L to μg/L [8,9]. Wastewater which often contains antibiotics with dozens or hundreds μg/L [10] has been identified as the main pollution source for antibiotics in waters [8,11]. It is necessary to treat wastewater containing antibiotics in terms of pollution source control. Sulfathiazole, a kind of sulfonamide antibiotics with short-acting functions, has been solely or jointly used for treating infections [12]. Sulfathiazole as well as the other sulfonamide antibiotics will cause potential risks and pathogenic bacteria drug-resistance even at the low concentration [11] so that the removal of

---

sulfonamide antibiotics has been widely studied.

Many techniques including bioremediation [13], photo-degradation [14], biochar adsorption [15], reverse osmosis nanofiltration [16], and advanced oxidation processes [17–19] have been developed for removing antibiotics from aqueous environments. Compared with the other methods, advanced oxidation processes (AOPs) have shown the excellent advantages such as fast reaction, relatively low cost, and high removal efficiency. Among different AOPs, catalytic ozonation is a promising approach for removing the recalcitrant pollutants due to rapid reaction rate and gentle reaction conditions [3]. More attention has been recently paid for developing different catalysts since they are critical for catalytic ozonation [3,4,20]. Magnetic $Mg(OH)_2$ ($Fe_3O_4@Mg(OH)_2$) prepared by bischofite is proved as an effective catalyst with easy separation feature for ozonation of antibiotics [3]. However, catalytic activity of $Fe_3O_4@Mg(OH)_2$ might decrease because Fe_3O_4 core is generally unstable, susceptible to corrode, and easy to agglomerate. Therefore, SiO_2 layer can protect and stabilize Fe_3O_4 core to improve magnetic $Mg(OH)_2$ catalyst. Little information on $Fe_3O_4@SiO_2@Mg(OH)_2$ catalyst is provided.

Therefore, this study prepared $Fe_3O_4@SiO_2@Mg(OH)_2$ catalyst for catalytic ozonation of sulfathiazole by using the waste bischofite from salt industry. The micro morphology, characteristics, and functional groups of synthesized catalyst were discussed. Moreover, the effect of different conditions, mineralization and antibacterial activity, and possible degradation pathways of target antibiotic during catalytic ozonation by synthesized $Fe_3O_4@SiO_2@Mg(OH)_2$ were also explored. The final goal of this study was to provide the new promising recycling pathway of waste bischofite.

2. Materials and methods

2.1. Chemicals and Preparation of $Fe_3O_4@SiO_2@Mg(OH)_2$

Chemicals including tetraethyl orthosilicate (TEOS), hexadecyl-trimethylammonium bromide (CTAB), tert-butanol (TBA), ethylene glycol, ferric chloride ($FeCl_3·6H_2O$), sodium acetate (CH_3COONa), $NaHCO_3$, Na_2SO_4, sodium thiosulphate ($Na_2S_2O_3$), polyethylene glycol (PEG)10000, C_2H_5OH, HCl, $NH_3·H_2O$, and salts (NaCl, $CaCl_2$, and $MgCl_2$) were of analytical purity, purchased from Sinopharm Chemical Reagent Co. Ltd. (Shanghai, China), and used without further purification. Sulfathiazole with purity > 98% was purchased from TCI Chemicals (Shanghai, China). Acetonitrile of HPLC (high performance liquid chromatography) grade was obtained from Mreda (Columbia, MD, USA). Natural bischofite used for catalyst synthesis was collected from the Qarhan Salt Lake of China (Fig. 1).

Magnetic core-shell $Fe_3O_4@SiO_2@Mg(OH)_2$ nano-composite was synthesized by the following steps. Firstly, solvothermal method was used to synthesize magnetic Fe_3O_4 microspheres [21]. Ethylene glycol (40 mL) was used to solve $FeCl_3·6H_2O$ (1.35 g), CH_3COONa (3.6 g), and PEG 10000 (1.0 g) under vigorous magnetic stirring at room temperature for 1 h to obtain uniform yellow mixture solution. The mixture was then placed in the Teflon-lined stainless-steel reactive autoclave, sealed, heated at 200 °C for 10 h, and then naturally cooled down to room temperature to obtain the black products which were separated using a permanent magnet, washed several times by distilled water and ethanol, and dried at 60 °C for 12 h. Secondly, core-shell $Fe_3O_4@SiO_2$ microspheres were synthesized by sol-gel method [22]. Total 50 mL of HCl aqueous solution with concentration of 0.1 mol/L was added into the Fe_3O_4 particles with 0.1 g and sonicated for 10 min. The magnetic particles which were separated by permanent magnet and washed by distilled water were then uniformly dispersed in a mixture solution of ethanol (80 mL), distilled water (20 mL) and 1.0 mL of concentrated ammonia aqueous solution (28% wt). TEOS (30 μL) was added into the above mixture solution drop by drop under vigorous magnetic stirring at room temperature for 6 h to obtain the $Fe_3O_4@SiO_2$ microspheres which were separated, washed several times with distilled water and

ethanol, and dried at 60 °C for 12 h. Finally, a chemical precipitation method was used to deposit $Mg(OH)_2$ shell on the surface of $Fe_3O_4@SiO_2$ core. $Fe_3O_4@SiO_2$ particles (0.1 g) were dissolved in 30 mL of CTAB solution (0.15 g) and ultrasonically treated for 30 min. The 3.4 mL of $MgCl_2$ solution (0.5 mol/L) was slowly added into the above solution and stirred for 1 h at room temperature. $NH_3·H_2O$ (260 μL) was added to the above solution under constant mechanical stirring and the solution was heated at 50 °C for 4 h. Then the solution was naturally cooled down to room temperature to obtain the target products which were separated with a magnet, rinsed several times with ethanol, and dried at 60 °C.

2.2. Ozonation experiments

The sulfathiazole ozonation experiments were conducted in a three-necked round-bottomed flask that contained 100 mL aqueous sulfathiazole solution with concentration of 50 mg/L and a certain amount of catalyst at 25 ± 2 °C. Ozone was produced by an ozone generator (Wohuan Co., Ltd) from high-purity oxygen and continuously fed into the bottom of the solution through a glass diffuser at a flow rate of 0.1 L/min and concentration of 0.5 g/h. $Na_2S_2O_3$ served as quencher for residual ozone and TBA was used as radical scavenger. The samples were collected at different intervals and residual ozone was quenched immediately with $Na_2S_2O_3$ solution. The samples were filtered through the 0.22 μm filter film for further analysis.

To discuss the removal efficiencies of sulfathiazole by different ozonation systems, the control experiments were performed at catalyst dosage of 0.15 g/L with initial sulfathiazole concentration of 50 mg/L under the conditions of ozonation alone, catalytic ozonation with Fe_3O_4, catalytic ozonation with $Mg(OH)_2$, and catalytic ozonation with $Fe_3O_4@SiO_2@Mg(OH)_2$. Adsorption of sulfathiazole on the synthesized $Fe_3O_4@SiO_2@Mg(OH)_2$ was also studied by using the oxygen to replace ozone with the remaining conditions same as ozonation experiments. This study discussed the effects of several factors on sulfathiazole removal by setting the catalyst dosage (0, 0.15, 0.3, 0.6, and 1.0 g/L), initial sulfathiazole concentration (10, 30, 50, 100, and 200 mg/L), and reaction temperature (15, 25, and 35 °C), respectively. Moreover, the pH of the aqueous solution was not adjusted except exploring the effect of pH on sulfathiazole removal with pH values of 3.0, 5.0, 7.0, 9.0, and 11.0. The effect of ions on sulfathiazole removal was also explored by setting different concentrations (0, 0.005, 0.05, 0.2, and 0.5 mol/L) of sodium salts (Cl-, HCO_3- and SO_4^{2-}) for anions and different concentrations (0, 0.005, 0.05, 0.2, and 0.5 mol/L) of chloride (Ca^{2+} and Mg^{2+}) for cations. TBA with concentration of 0.1 mol/L was used as hydroxyl radical scavenger.

Each assay was carried out in triplicate with result expressed by the mean values with standard deviations. The used catalyst was separated by an external magnetic field, washed, and dried. The gathered catalyst was directly reused in a fresh sulfathiazole solution for 4 times to test the stability of $Fe_3O_4@SiO_2@Mg(OH)_2$ catalyst.

2.3. Antibacterial activity of ST affected by catalytic ozonation

Toxicity to *Escherichia coli (E. coli) DH5α* viability was used to discuss the antibacterial activity of sulfathiazole before and after catalytic ozonation. *E. coli* was cultivated in the sterilized Luriae-Bertani (LB) medium (tryptone 10 g/L, yeast extract 5 g/L, NaCl 10 g/L). The LB medium diluted by 3 folds was sterilized at 121 °C for 30 min. The LB medium containing *E. coli* and sulfathiazole solution with tested concentration of 50 mg/L before and after catalytic ozonation was cultivated at 30 °C. Control assay was performed by using the same medium without sulfathiazole solution. The sample was taken within 24 h during the antibacterial activity experiment to measure the optical density at 600 nm (OD600 nm). The experiments were performed in triplicate.
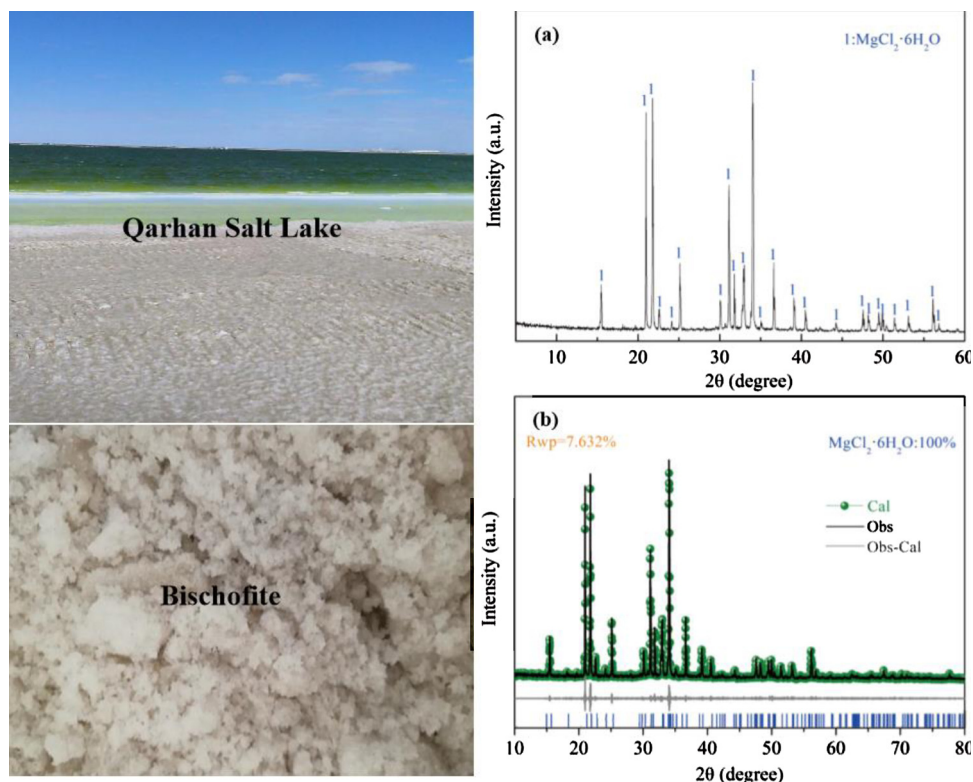
Fig. 1. Bischofite used for catalyst synthesis was collected from the Qarhan Salt Lake. The main content of the bischofite was identified using the standard X-ray diffraction patterns of $MgCl_2 \cdot 6H_2O$ by peak position (a) and peak intensity (b).

2.4. Instrumental Analysis

Scanning electron microscope (SEM, Hitachi S-4800, Japan), transmission electron microscope (TEM, JEM-1200EX, Japan) operating at 120 kV, and high-resolution transmission electron microscope (HRTEM, Tecnai G2 F20 S-TWIN, USA) working at 200KV were used to observe the morphology of the prepared materials. Tecnai G2 F20 S-TWIN (200 KV) high-angle annular dark-field scanning transmission electron microscope (HAADF-STEM) was used to obtain the HAADF-STEM images. X-ray diffraction patterns (XRD, Bruker D8, Germany) using a Co Kα irradiation with 2θ value in the range of 5°-90° was adopted to explore the crystalline phase of the samples. Fourier Transform Infrared Spectroscopy (FTIR, Nicolet IS10, American) at the wave numbers ranging from 400 to 4000 cm^{-1} was used to discuss the functional groups on the surface of samples. Surface and metal oxidation state of prepared materials were determined by an X-ray photoelectron spectrum (XPS, Thermo Scientific Escalab 250Xi) at a vacuum pressure ($< 10^{-7}$ Pa) with Al Kα X-ray excitation source. The magnetic properties of the samples were performed at room temperature using a Versalab vibrating sample magnetometer. The pH at the point of zero charge (pHpzc) was measured by using Zetasizer Nano S (Malvern Instruments, Malvern, UK). The total organic carbon (TOC) of the water samples was monitored by a TOC analyzer (TOC VCPH, Shimadu, Japan). The concentration of ozone was determined by bubbling the ozone gas stream into the 2% KI solution and analyzing the solution by iodometric titration method [23]. The optical density at 600 nm (OD600 nm) was measured with a UV-vis spectrophotometer (TU1810, Beijing Purkinje General Instrument Co., LTD, China).

HPLC (Wufeng Co., Shanghai, China) equipped with a UV detector and a C18 reversed-phase column (Waters SunFire, 2.1 × 150 mm, 3.5 μm) was used to determine the sulfathiazole concentrations. Sulfathiazole was measured under the conditions of the mobile phase of a mixture of water and acetonitrile (90:10 with the volume ratio), a flow rate of 0.2 mL/min, the column temperature of 30 °C, injection

volume of 5 μL, and the UV absorbance wavelength of 270 nm. The degradation products of sulfathiazole were identified using liquid chromatography-ion trap mass spectrometry (LCQ Fleet, ThermoFisher, USA) equipped with Waters SunFire C18 reversed-phase column (2.1 × 150 mm, 3.5 μm). The mobile phase conditions were similar to those used in the HPLC system, while the flow rate was 0.1 mL/min and the injection volume was 100 μL. The MS analysis was performed in positive and negative modes using electrospray ionization with spray voltage of 5 kV and a collision energy of 35 eV.

The kinetics of sulfathiazole ozonation catalyzed by $Fe_3O_4@SiO_2@Mg(OH)_2$ were evaluated using the pseudo-first-order kinetic model (Eq. (1)):

$$\ln C_t = \ln C_0 - kt \tag{1}$$

where C_0/C_t represents the initial/residual sulfathiazole concentrations at $0/t$ min; k is the pseudo first-order removal rate constant.

3. Results and discussion

3.1. Characterization of synthesized $Fe_3O_4@SiO_2@Mg(OH)_2$ catalyst

The main content of the natural bichofite was identified as $MgCl_2 \cdot 6H_2O$ using the standard XRD patterns of $MgCl_2 \cdot 6H_2O$ (Fig. 1). The SEM images of the synthesized samples showed that Fe_3O_4 particles were approximately-monodisperse spherical and $Fe_3O_4@SiO_2$ particles were still well-dispersed spherical even after loading SiO_2 on the surface of Fe_3O_4 microspheres (Figs. 2a-2b). In contrast, the SEM images of the $Fe_3O_4@SiO_2@Mg(OH)_2$ sample illustrated that many little $Mg(OH)_2$ nanoplates were adhered to the surface of the $Fe_3O_4@SiO_2$ microspheres to make the surfaces rough (Fig. 2c). The TEM images further confirmed the monodisperse spherical micromorphology of Fe_3O_4 and $Fe_3O_4@SiO_2$ (Figs. 2d-2e). The dark parts on the TEM image of $Fe_3O_4@SiO_2$ might be ascribed to the high electron density of the Fe_3O_4 particles while the brightness and low-darkness areas indicated that SiO_2
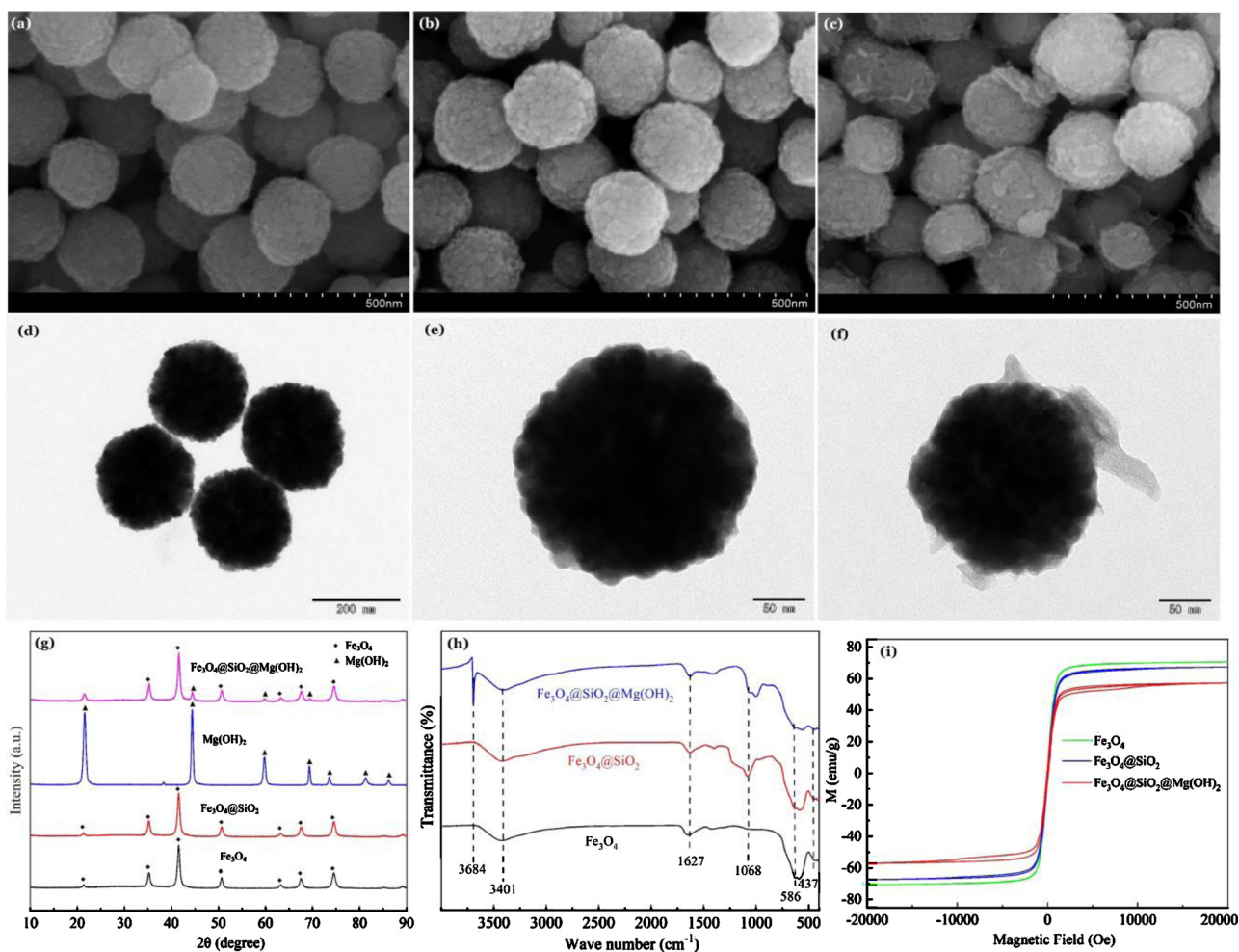
Fig. 2. SEM images of Fe_3O_4 (a), $Fe_3O_4@SiO_2$ (b), and $Fe_3O_4@SiO_2@Mg(OH)_2$ (c), TEM images of Fe_3O_4 (d), $Fe_3O_4@SiO_2$ (e), and $Fe_3O_4@SiO_2@Mg(OH)_2$ (f), XRD patterns (g), FTIR spectra (h), and magnetic hysteresis loops (i) of the synthesized materials.

layer was very thin (Fig. 2e). The TEM image of $Fe_3O_4@SiO_2@Mg(OH)_2$ (Fig. 2f) clearly exhibited that the outermost layer was composed of Mg $(OH)_2$ nanoplates and the synthesized microspheres became lighter than Fe_3O_4 and $Fe_3O_4@SiO_2$. These results clearly suggested that SiO_2 and $Mg(OH)_2$ layer was uniformly deposited on the surface of Fe_3O_4 microspheres.

The XRD pattern of the $Fe_3O_4@SiO_2$ was very similar to that of the Fe_3O_4 (Fig. 2g). Characteristic diffraction peaks corresponding to SiO_2 were not detected because the SiO_2 loaded on Fe_3O_4 was amorphous, which was similar to the previous report [24]. All the characteristic diffraction peaks of synthesized $Fe_3O_4@SiO_2@Mg(OH)_2$ were assigned to pure phase of $Mg(OH)_2$ in addition to the Fe_3O_4 reflections (Fig. 2g). The typical (101), (102) and (110) peaks of the $Mg(OH)_2$ were distinctly observed, indicating the high crystallinity of the synthesized composite. Many important functional groups existed on the surface of the synthesized materials based on the strong peaks of the FTIR spectra (Fig. 2h). All materials possessed a strong broad band around 3401 cm^{-1} assigning to hydroxyl groups due to the physical adsorption of molecular water and band around 1627 cm^{-1} due to their bending mode [25,26]. The FTIR spectra of Fe_3O_4 possessed a broad band at 586 cm^{-1} assigned to Fe-O stretching vibration while that of $Fe_3O_4@SiO_2$ had an additional peak around 1068 cm^{-1} related to stretching vibration of Si-O bond of silica [24,26]. The FTIR spectra of $Fe_3O_4@SiO_2@Mg(OH)_2$ possessed all above-mentioned peaks as well as the strong peak at 3684 cm^{-1} related to O-H stretching vibration in the crystal structure of Mg $(OH)_2$ and peak around 437 cm^{-1} assigned to the Mg-O stretching vibration, illustrating that SiO_2 and $Mg(OH)_2$ were successfully deposited

on Fe_3O_4. The magnetic hysteresis loops showed that the saturation magnetization value (Ms) of Fe_3O_4, $Fe_3O_4@SiO_2$, and $Fe_3O_4@SiO_2@Mg$ $(OH)_2$ was about 70.5, 67.4, and 57.3 emu/g, respectively (Fig. 2i). The existence of external layer of amorphous SiO_2 might make Ms value of $Fe_3O_4@SiO_2$ composite slightly lower than that of pure Fe_3O_4. Accordingly, amorphous SiO_2 and outermost non-magnetic $Mg(OH)_2$ caused the Ms value of $Fe_3O_4@SiO_2@Mg(OH)_2$ composite to be much lower than that of Fe_3O_4 and $Fe_3O_4@SiO_2$. Similar with the previous report [3], the synthesized $Fe_3O_4@SiO_2@Mg(OH)_2$ composite could be easily separated from aqueous solution using an external magnetic field to show excellent magnetic responsiveness and redispersibility for the practical usage or manipulation.

The HRTEM image of $Fe_3O_4@SiO_2@Mg(OH)_2$ composite illustrated that this synthesized material possessed core-shell structure (Fig. 3a). HAADF-STEM image exhibited that the difference in the central region and the outer region further confirmed the core-shell structure of $Fe_3O_4@SiO_2@Mg(OH)_2$ composite (Fig. 3b). Element mapping also showed that this composite microsphere was composed of a Fe_3O_4 core, a SiO_2 shell and a $Mg(OH)_2$ outer shell (Fig. 3c-3e). EDS line scan of $Fe_3O_4@SiO_2@Mg(OH)_2$ showed that the synthesized composite was composed of Fe_3O_4, SiO_2, and $Mg(OH)_2$ (Fig. 3f). Mg (1 s), Fe (2p), O (1 s) and Si (2p) existed on the XPS survey scan of $Fe_3O_4@SiO_2@Mg(OH)_2$ (Fig. 3g). The peak in the region of 720-705 eV came from Fe 2p3/2 and that in the range of 735-720 eV were from Fe 2p1/2 for Fe 2p spectra of $Fe_3O_4@SiO_2@Mg(OH)_2$ (Fig. 3h), suggesting the existence of Fe_3O_4. The binding energies of Fe 2p3/2 for Fe^{2+} and Fe^{3+} were 710.4 eV and 712.6 eV, respectively (Fig. 3h). The O1 s peaks of $Fe_3O_4@SiO_2@Mg$
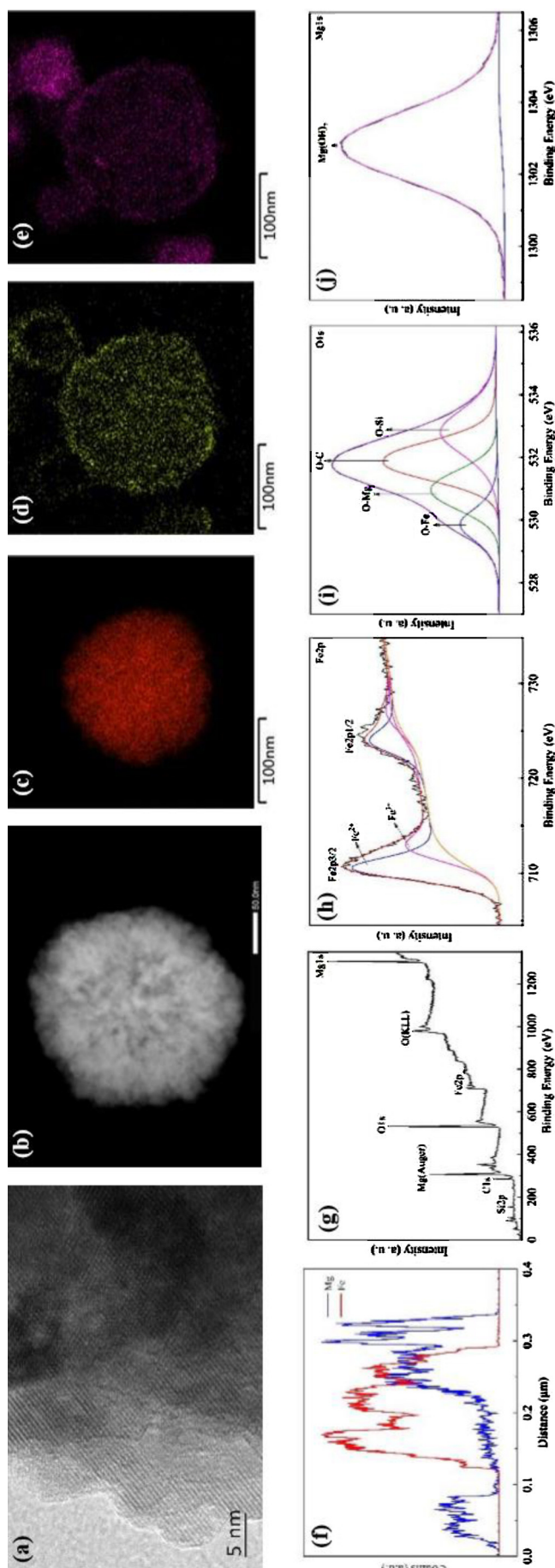
Fig. 3. HRTEM image (a), HAADF-STEM image (b), Fe mapping (c), Mg mapping (d), Si mapping (d), Mg mapping (e), EDS line scans (f), XPS survey scan (g), Fe 2p (h), O 1s (d), and Mg 1s (e) of synthesized $Fe_3O_4@SiO_2@Mg(OH)_2$.

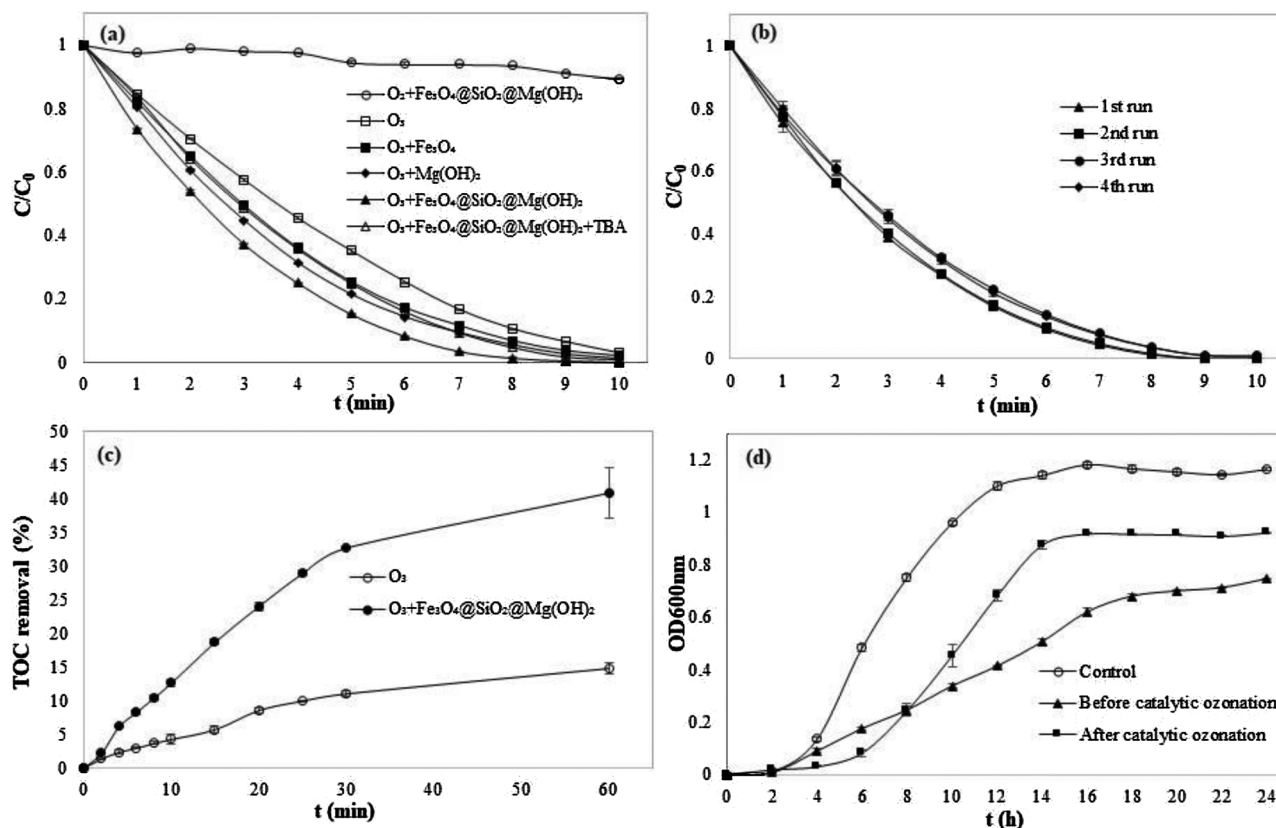**Fig. 4.** Sulfathiazole degradation under different conditions (a), catalytic ozonation performance of $Fe_3O_4@SiO_2@Mg(OH)_2$ in successive runs (b), mineralization of sulfathiazole in catalytic ozonation by $Fe_3O_4@SiO_2@Mg(OH)_2$ (c), and variation of antibacterial activity in catalytic ozonation by $Fe_3O_4@SiO_2@Mg(OH)_2$ (d).

$(OH)_2$ were located at 529.8 eV attributed to the lattice oxygen on the surface of metal oxides (O-Fe), 530.9 eV assigned to chemisorbed oxygen groups or surface hydroxyl group (O-Mg), and 532.8 eV assigned to the oxygen bonding with Si atoms (O-Si), respectively (Fig. 3i). Furthermore, the peak at 1302.7 eV was assigned to Mg1 s of $Mg(OH)_2$ based on Mg 1 s spectra of $Fe_3O_4@SiO_2@Mg(OH)_2$ (Fig. 3j). These results further exhibited the core-shell structure and composition of the synthesized $Fe_3O_4@SiO_2@Mg(OH)_2$.
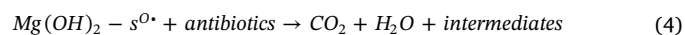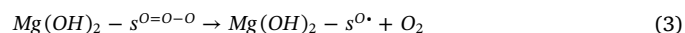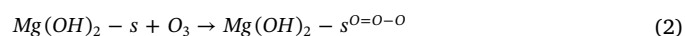
3.2. Sulfathiazole degradation under different oxidation conditions

Sulfathiazole could be rapidly removed by ozonation process (Fig. 4a). Approximately 97.2%/98.0%/98.8%/99.9% of sulfathiazole was removed by single ozonation/catalytic ozonation by Fe_3O_4/catalytic ozonation by $Mg(OH)_2$/catalytic ozonation by $Fe_3O_4@SiO_2@Mg(OH)_2$ process within 10 min (Fig. 4a). Adsorption of sulfathiazole on $Fe_3O_4@SiO_2@Mg(OH)_2$ was lower than 11%, illustrating that most of sulfathiazole was removed by catalytic ozonation. The reaction rate constant of sulfathiazole was 0.286/0.338/0.375/0.542 min^{-1} with R^2 = 0.97/0.98/0.95/0.95 during process of single ozonation/catalytic ozonation by Fe_3O_4/catalytic ozonation by $Mg(OH)_2$/catalytic ozonation by $Fe_3O_4@SiO_2@Mg(OH)_2$, suggesting that this core-shell material possessed more excellent catalytic ozonation capacity than Fe_3O_4 and $Mg(OH)_2$. Reaction rate constant of sulfathiazole in catalytic ozonation by $Fe_3O_4@SiO_2@Mg(OH)_2$ was almost double that of single ozonation and 1.5 times that of catalytic ozonation by Fe_3O_4 or $Mg(OH)_2$, which might be ascribed to high specific surface area (66.982 m^2/g) of this core-shell material. Moreover, SEM images showed that many small Mg $(OH)_2$ nanoplates were distributed on the surface of $Fe_3O_4@SiO_2@Mg$ $(OH)_2$ to provide reaction active sites for catalytically ozonizing sulfathiazole. The previous studies also reported the similar improvement due to large specific surface area [3]. Many hydroxyl groups which
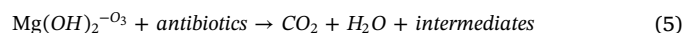
could provide initiators for ozonation [25] existed on the surface of the $Fe_3O_4@SiO_2@Mg(OH)_2$ catalyst based on the FTIR spectrum (Fig. 2h). Therefore, TBA was used as hydroxyl radical scavenger to discuss the possible reaction mechanism (Fig. 4a). The reaction constant of sulfathiazole during catalytic ozonation by $Fe_3O_4@SiO_2@Mg(OH)_2$ in the presence of TBA (0.397 min^{-1}, R^2 = 0.9) decreased by 26.8% compared with that without TBA (0.542 min^{-1}, R^2 = 0.95), illustrating that hydroxyl radical reaction route was partly engaged in the catalytic ozonation of sulfathiazole during catalytic ozonation by $Fe_3O_4@SiO_2@Mg$ $(OH)_2$. Besides the hydroxyl radical oxidation, other removal mechanisms occurring both on the catalyst surfaces and in the bulk solution might also have been involved in the process of ozonation (Fig. 5). According to the catalytic ozonation of phenol using MgO as catalyst [27], the mechanisms were proposed for the catalytic ozonation by $Fe_3O_4@SiO_2@Mg(OH)_2$.

On the surface of the catalyst:
Radical type catalytic oxidation

$$Mg(OH)_2 - s + O_3 \rightarrow Mg(OH)_2 - s^{O=O-O} \tag{2}$$

$$Mg(OH)_2 - s^{O=O-O} \rightarrow Mg(OH)_2 - s^{O\bullet} + O_2 \tag{3}$$

$$Mg(OH)_2 - s^{O\bullet} + antibiotics \rightarrow CO_2 + H_2O + intermediates \tag{4}$$

Direct oxidation with ozone molecules

$$Mg(OH)_2{}^{-O_3} + antibiotics \rightarrow CO_2 + H_2O + intermediates \tag{5}$$

In the bulk solution:
Direct oxidation with ozone molecules

$$O_3 + antibiotics \rightarrow CO_2 + H_2O + intermediates \tag{6}$$

On the surface of nano-$Mg(OH)_2$, ozone molecules could form hydrogen bounds with the hydroxyl groups (Eq.(2)). The bounded ozone then partly decomposed to atomic oxygen (Eq.(3)), which accelerated
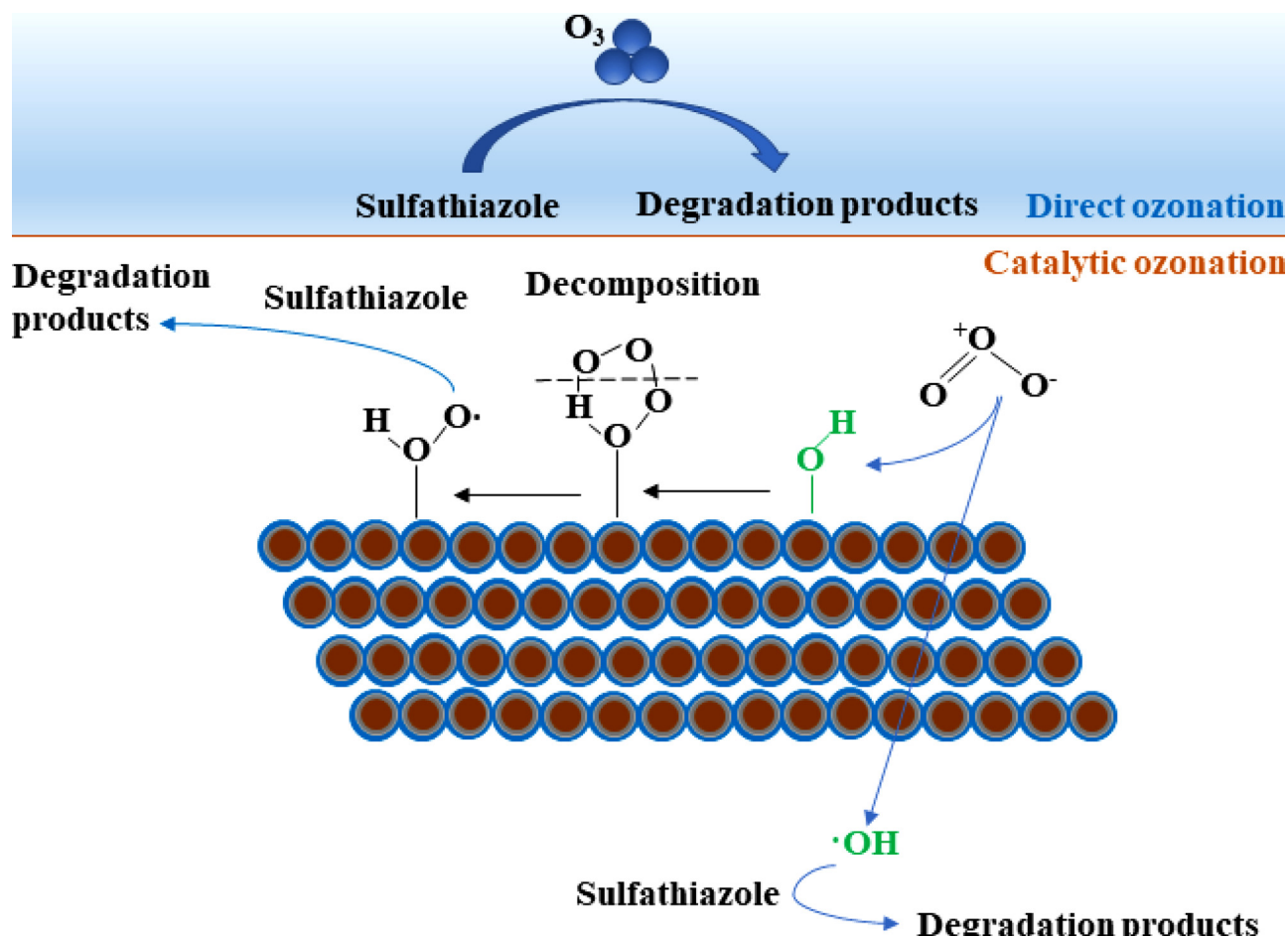
Fig. 5. Proposed mechanisms for the removal of sulfathiazole using $Fe_3O_4@SiO_2@Mg(OH)_2$.

the catalytic ozonation of sulfathiazole (Eq.(4)). Undissociated ozone bounded with the catalyst also directly oxidized the antibiotic in contact with it (Eq.(5)). Additionally, ozone and sulfathiazole solubilized in the solution could directly react with each other in the bulk solution, resulting into partial degradation of the sulfathiazole (Eq.(6)).

Synthesized $Fe_3O_4@SiO_2@Mg(OH)_2$ catalyst could be easily separated by extra magnetic field and used without further treatment. The used $Fe_3O_4@SiO_2@Mg(OH)_2$ catalyst still possessed good stability after reused several times (Fig. 4b). About 99.0% of sulfathiazole could be removed by catalytic ozonation with $Fe_3O_4@SiO_2@Mg(OH)_2$ that was reused 4 times, which exhibited that the $Fe_3O_4@SiO_2@Mg(OH)_2$ catalyst possessed better stability and recyclability that many previously-reported catalysts [4,20]. In contrast, demagnetization frequently occurs when reusing Fe_3O_4 catalyst which is generally unstable due to co-existence of Fe^{2+} and Fe^{3+} while it is very difficult to separate Mg(OH)₂ especially nano-Mg(OH)₂ from solution. Catalytic ozonation using $Fe_3O_4@SiO_2@Mg(OH)_2$ possessed higher reaction rate in comparison with single ozonation as well as catalytic ozonation with Fe_3O_4 or $Mg(OH)_2$ and $Fe_3O_4@SiO_2@Mg(OH)_2$ also showed more excellent stability and recyclability, proving that the synthesized $Fe_3O_4@SiO_2@Mg(OH)_2$ was a promising catalyst for ozonation of antibiotics.

3.3. Mineralization and antibacterial activity of sulfathiazole influenced by catalytic ozonation by synthesized $Fe_3O_4@SiO_2@Mg(OH)_2$

The mineralization process of sulfathiazole during catalytic ozonation by synthesized $Fe_3O_4@SiO_2@Mg(OH)_2$ catalyst was evaluated by TOC removal (Fig. 4c). Only 14.5% of TOC was removed during the single ozonation process after 60-min treatment while approximately

40.1% of TOC was removed within 60 min by catalytic ozonation with $Fe_3O_4@SiO_2@Mg(OH)_2$, suggesting that the presence of $Fe_3O_4@SiO_2@Mg(OH)_2$ would enhance the mineralization of sulfathiazole. The formation of typical radicals could be accelerated by adding catalyst to subsequently enhance the degradation of target antibiotics [3], which could also explain the results of this research work. Interestingly, the TOC removal percentage of sulfathiazole within 60 min in the presence of $Fe_3O_4@SiO_2@Mg(OH)_2$ was lower than that of metronidazole with catalytic ozonation by $Fe_3O_4@Mg(OH)_2$ [3], exhibiting that mineralization of different antibiotics in catalytic ozonation by different catalysts might be influenced by various factors.

The antibacterial activity of sulfathiazole after and before the catalytic ozonation by $Fe_3O_4@SiO_2@Mg(OH)_2$ was evaluated (Fig. 4d). *E. coli* growth was seriously inhibited when sulfathiazole existed with high concentration (50 mg/L) while that was effectively ameliorated after catalytic ozonation, suggesting that catalytic ozonation played important role in affecting antibacterial activity of sulfathiazole. Similar observations were also reported by the other study [3].

3.4. Catalytic ozonation of sulfathiazole by synthesized $Fe_3O_4@SiO_2@Mg(OH)_2$ under different environmental conditions

Catalytic ozonation of sulfathiazole by synthesized $Fe_3O_4@SiO_2@Mg(OH)_2$ was affected by different environmental conditions (Fig. 6). Addition of catalyst could significantly increase the ozonation rate of sulfathiazole (Fig. 6a). About 96.4%/94.0% of sulfathiazole was removed within 7 min with catalyst dose of 0.15/0.30 g/L while the removal efficiency was comparable with that of single ozonation when dose further increased. The reaction rate constant of sulfathiazole with
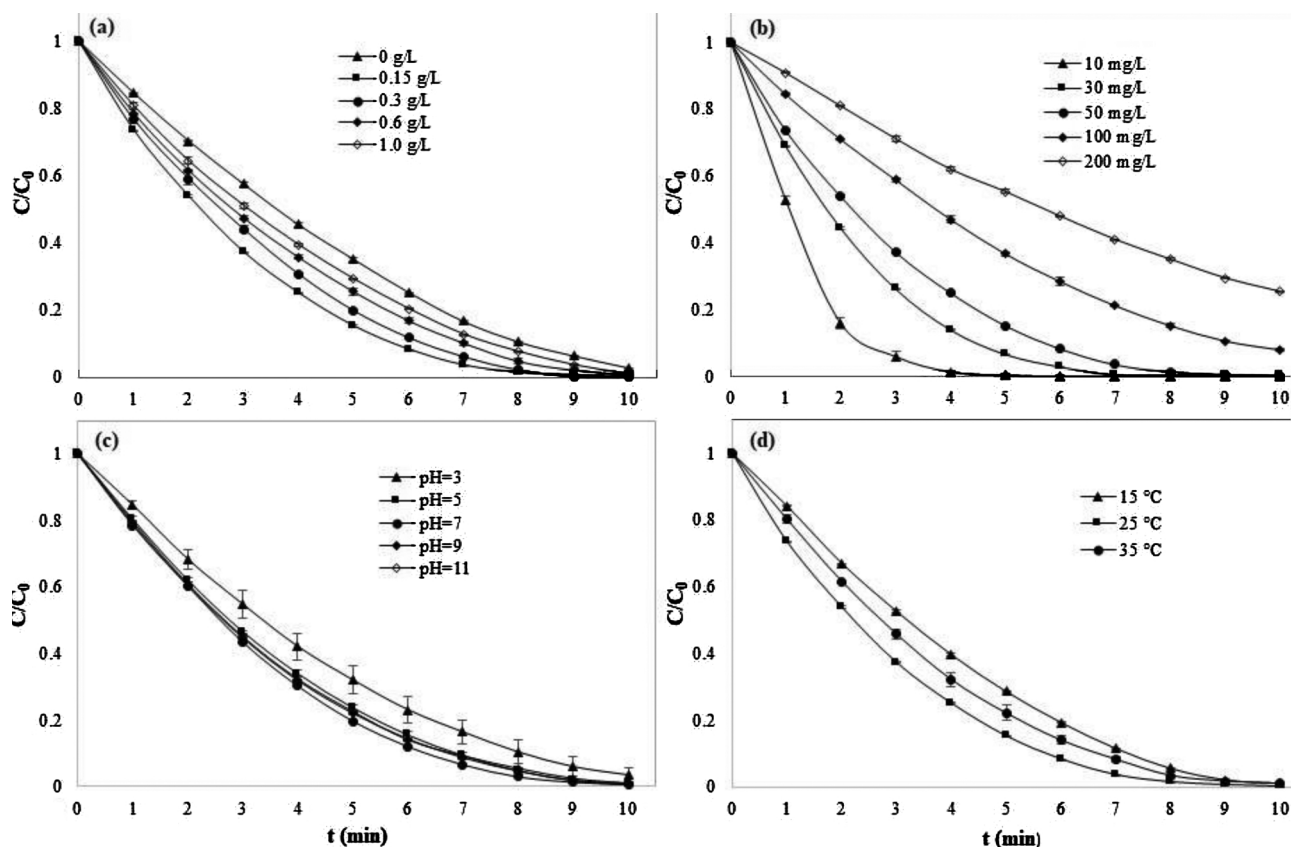
Fig. 6. Effect of catalyst dosage (a), initial concentration (b), initial pH (c) and reaction temperature (d) on catalytic ozonation of sulfathiazole by $Fe_3O_4@SiO_2@Mg(OH)_2$.

catalyst dose of 0.15/0.3/0.6/1.0 g/L was approximately 1.9/2.0/1.4/1.2 times that under single ozonation. Removal rate of sulfathiazole with catalyst dosage less than 0.15 g/L was lower than that with 0.15 g/L based on the results of pre-experiment. Considering fast degradation of sulfathiazole during the first 7 min and treatment cost, 0.15 g/L might be the optimal dosage for catalytic ozonation of sulfathiazole.

Initial contaminant concentration significantly affected the reaction efficiency and rate of catalytic ozonation (Fig. 6b). Low initial concentration generally obtained higher removal efficiency and rate due to more active sites and enough contact among ozone and contaminant. The reaction rate constant reached 0.849/0.635 min^{-1} with R^2 = 0.97/0.98 and the initial concentration of 10/30 mg/L, almost 1.6/1.2 times that with initial concentration of 50 mg/L. In contrast, the reaction rate constant decreased to 0.232/0.130 min^{-1} with R^2 = 0.99/0.99 when treating 100/200 mg/L sulfathiazole solution. The catalytic ozonation was faster within the initial 7 min at relatively low concentration and about 99.9%/99.6%/96.4% of sulfathiazole was removed. However, high initial concentrations clearly inhibited the ozonation rate with only 78.8%/59.0% of sulfathiazole was removed within 7 min at concentration of 100/200 mg/L.

Effect of pH on catalytic ozonation of sulfathiazole by synthesized $Fe_3O_4@SiO_2@Mg(OH)_2$ was not very significant compared with catalyst dose and initial concentration (Fig. 6c). Except pH of 3.0 that negatively influenced the ozonation efficiency, the removal rate at pH range of 5-11 was higher than 90.6% within 7 min or higher than 99.1% within 10 min. The reaction rate constant of sulfathiazole at pH of 5.0/7.0/9.0/11.0 was 1.4/1.5/1.4/1.3 times that at pH of 3.0, illustrating that neutral condition was the optimal for catalytic ozonation of sulfathiazole using synthesized $Fe_3O_4@SiO_2@Mg(OH)_2$. Adjustment of pH generally adds the wastewater treatment cost. Therefore, the synthesized catalyst was a promising material in terms of ozonation process.

The ozonation reaction rate constant of sulfathiazole reached 0.368/0.542/0.406 min^{-1} with R^2 = 0.95/0.95/0.97 at 15/25/35 °C, suggesting that 25 °C should be the optimal temperature for catalytic ozonation of sulfathiazole using synthesized $Fe_3O_4@SiO_2@Mg(OH)_2$. This result might be explained by the competition of opposite effects that high temperature would increase chemical reaction rate and decrease the ozone solubility to reduce the formation of hydroxyl radicals [28]. Optimal temperature of 25 °C further confirmed that the synthesized $Fe_3O_4@SiO_2@Mg(OH)_2$ was promising since no extra heating or cooling for ozonation was needed to reduce the treatment cost.

3.5. Effects of inorganic ions on catalytic ozonation of sulfathiazole by synthesized $Fe_3O_4@SiO_2@Mg(OH)_2$

Similar with the previous study [3,4], the inorganic anions posed negative effect on catalytic ozonation of sulfathiazole by synthesized $Fe_3O_4@SiO_2@Mg(OH)_2$ (Figs. 7a-7c). Compared with control (no anion addition), the reaction rate constant of catalytic ozonation decreased by 37.9%-47.1% with Cl- addition concentration in the range of 0.005-0.5 mol/L (Fig. 7a). Accordingly, the reaction rate constant decreased by 45.8%-58.3% for SO_4^{2-} addition (Fig. 7b) and by 34.1%-65.8% for HCO_3- addition (Fig. 7c). Increase in anion addition concentration decreased reaction rate, especially for HCO_3-. These results might be explained by that anions would be adsorbed on the surface of catalyst and occupied the active sites to inhibit the ozonation process.

Inorganic cations also showed the similar negative effects on the catalytic ozonation of sulfathiazole (Figs. 7d-7e). Compared with control (no anion addition), the reaction rate constants of sulfathiazole decreased by 38.7%-50.7% with Ca^{2+} addition while those decreased by 32.9%-54.4% with Mg^{2+} addition. Effects of inorganic cations on ozonation could be ascribed to the role of corresponding anions (Cl- in this study) since cations did not participate in the ozonation reaction.
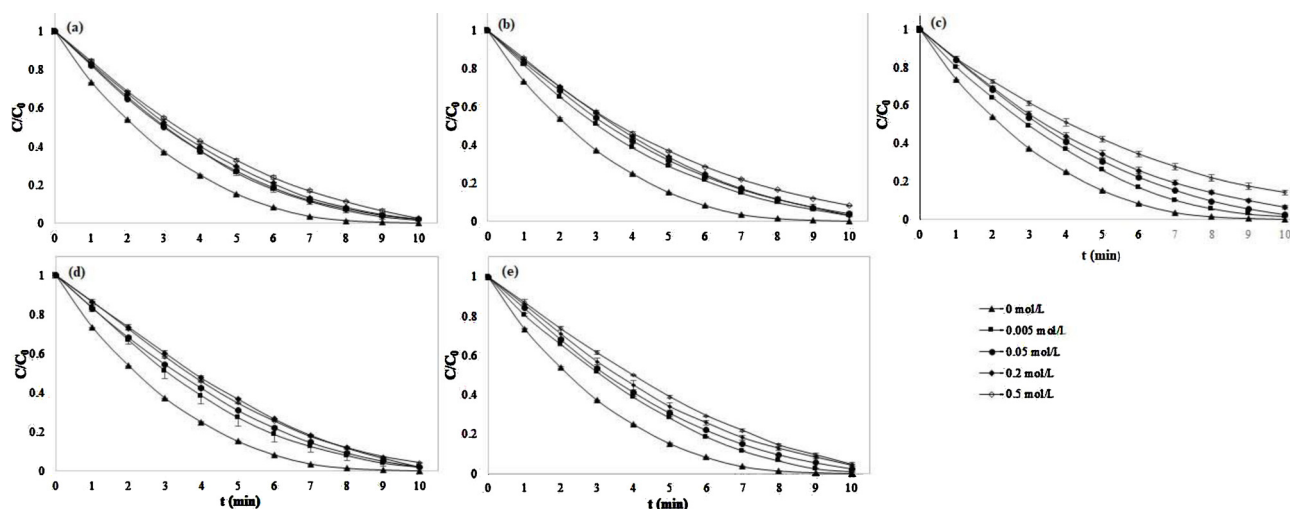
Fig. 7. Effect of inorganic anions including Cl- (a), SO_4^{2-} (b), and HCO_3^- (c) as well as cations including Ca^{2+} (d) and Mg^{2+} (e) on catalytic ozonation of sulfathiazole by $Fe_3O_4@SiO_2@Mg(OH)_2$.
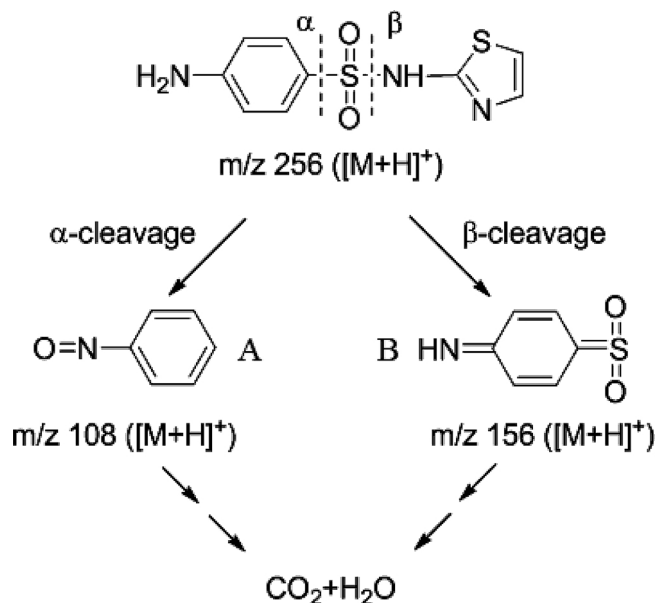

Fig. 8. Possible degradation pathway of sulfathiazole by catalytic ozonation with synthesized $Fe_3O_4@SiO_2@Mg(OH)_2$.

3.6. Possible degradation pathway of sulfathiazole by the catalytic ozonation with synthesized $Fe_3O_4@SiO_2@Mg(OH)_2$

Two main degradation products were formed during the catalytic ozonation of sulfathiazole (Fig. 8). One degradation product had a molecular ion of m/z 108 ([M+H]$^+$) while another product had a molecular ion of m/z 156 ([M+H]$^+$). Based on the product identification, the sulfathiazole was degraded through the cleavage of S-C bound or S-N bound, and the oxidation of the amino group (Fig. 8). Product A was formed through the cleavage of S-C bound and the oxidation of the amino group while product B was formed through the cleavage of S-N bound and the oxidation of the amino group. Product B could also be transformed from sulfamethoxazole in the Fe°/peroxymonosulfate oxidation system [29]. These products could be further transformed into CO_2 and H_2O.

4. Conclusions

The synthesized $Fe_3O_4@SiO_2@Mg(OH)_2$ catalyst was a core-shell nano-composite with magnetic responsiveness for easy separation. Sulfathiazole could be removed within 10 min by catalytic ozonation with $Fe_3O_4@SiO_2@Mg(OH)_2$. $Fe_3O_4@SiO_2@Mg(OH)_2$ showed excellent recyclability and stability to serve as a promising catalyst for catalytic ozonation of target compound. Catalytic ozonation could improve the mineralization of sulfathiazole and decrease its antibacterial activity. Initial concentration had significant effect on removal of sulfathiazole while neutral or alkaline conditions were appropriate for sulfathiazole removal. Catalyst dosage and temperature also influenced the removal of sulfathiazole to some extent. Inorganic cations and anions had negative effect on degradation of sulfathiazole. Cleavage and oxidation were the possible pathways of sulfathiazole degradation during catalytic ozonation. Good performance of removing sulfathiazole by catalytic ozonation using $Fe_3O_4@SiO_2@Mg(OH)_2$ suggested that this material might also serve as good catalyst for ozonation of the other organic pollutants such as sulfonamide antibiotics, pesticides, and hormones. The synthesized $Fe_3O_4@SiO_2@Mg(OH)_2$ particles using bischofite were promising for catalytic ozonation of target antibiotics.

References

[1] A. Gutierrez, S. Ushak, H. Galleguillos, A. Fernandez, L.F. Cabeza, M. Grágeda, Use of polyethylene glycol for the improvement of the cycling stability of bischofite as

thermal energy storage material, Appl. Energ. 154 (2015) 616–621.

[2] W. Liu, H. Xu, X. Shi, X. Yang, X. Wang, Improved Lime Method to Prepare High-Purity Magnesium Hydroxide and Light Magnesia from Bischofite, JOM 71 (2019) 4674–4680.

[3] J. Lu, Q. Sun, J. Wu, G. Zhu, Enhanced ozonation of antibiotics using magnetic Mg (OH)$_2$ nanoparticles made through magnesium recovery from discarded bischofite, Chemosphere 238 (2020) 124694.

[4] Q. Sun, J. Lu, J. Wu, G. Zhu, Catalytic ozonation of sulfonamide, fluoroquinolone, and tetracycline antibiotics using nano-magnesium hydroxide from natural bischofite, Water Air Soil Pollut. 230 (2019) 55.

[5] W.W. Cai, T. Peng, J.N. Zhang, L.X. Hu, B. Yang, Y.Y. Yang, J. Chen, G.G. Ying, Degradation of climbazole by UV/chlorine process: Kinetics, transformation pathway and toxicity evaluation, Chemosphere 219 (2019) 243–249.

[6] C.X. Hiller, U. Hübner, S. Fajnorova, T. Schwartz, J.E. Drewes, Antibiotic microbial resistance (AMR) removal efficiencies by conventional and advanced wastewater treatment processes: A review, Sci. Total Environ. 685 (2019) 596–608.

[7] W. Baran, E. Adamek, J. Ziemiańska, A. Sobczak, Effects of the presence of sulfonamides in the environment and their influence on human health, J. Hazard Mater. 196 (2011) 1–15.

[8] J. Lu, J. Wu, C. Zhang, Y. Zhang, Y. Lin, Y. Luo, Occurrence, distribution, and ecological-health risks of selected antibiotics in coastal waters along the coastline of China, Sci. Total Environ. 644 (2018) 1469–1476.

[9] I.T. Carvalho, L. Santos, Antibiotics in the aquatic environments: A review of the European scenario, Environ. Int. 94 (2016) 736–757.

[10] D.L. Cheng, H.H. Ngo, W.S. Guo, S.W. Chang, D.D. Nguyen, S.M. Kumar, B. Du, Q. Wei, D. Wei, Problematic effects of antibiotics on anaerobic treatment of swine wastewater, Bioresource Technol. 263 (2018) 642–653.

[11] W. Baran, J. Sochacka, W. Wardas, Toxicity and biodegradability of sulfonamides and products of their photocatalytic degradation in aqueous solutions, Chemosphere 65 (2006) 1295–1299.

[12] A. Pal, R. Gaba, S. Soni, Effect of presence of a-cyclodextrin and b-cyclodextrin on solution behavior of sulfathiazole at different temperatures: thermodynamic and spectroscopic studies, J. Chem. Thermodyn. 119 (2018) 102–113.

[13] M. Kumar, S. Jaiswal, K.K. Sodhi, P. Shree, D.K. Singh, P.K. Agrawal, P. Shukla, Antibiotics bioremediation: Perspectives on its ecotoxicity and resistance, Environ. Int. 124 (2019) 448–461.

[14] X.-Z. Niu, J. Glady-Croué, J.-P. Croué, Photodegradation of sulfathiazole under simulated sunlight: Kinetics, photo-induced structural rearrangement, and antimicrobial activities of photoproducts, Water Res. 124 (2017) 576–583.

[15] J. Wu, J. Lu, C. Zhang, Z. Zhang, X. Min, Adsorptive Removal of Tetracyclines and Fluoroquinolones Using Yak Dung Biochar, B, Environ. Contam. Tox. 102 (2019) 407–412.

[16] V. Homem, L. Santos, Degradation and removal methods of antibiotics from aqueous matrices - A review, J. Environ. Manage. 92 (2011) 2304–2347.

[17] R. Anjali, S. Shanthakumar, Insights on the current status of occurrence and removal of antibiotics in wastewater by advanced oxidation processes, J. Environ. Manage. 246 (2019) 51–62.

[18] P. Sun, Y. Li, T. Meng, R. Zhang, M. Song, J. Ren, Removal of sulfonamide antibiotics and human metabolite by biochar and biochar/H$_2$O$_2$ in synthetic urine, Water Res. 147 (2018) 91–100.

[19] B. Yang, R.S. Kookana, M. Williams, G.G. Ying, J. Du, H. Doan, A. Kumar, Oxidation of ciprofloxacin and enrofloxacin by ferrate(VI): Products identification, and toxicity evaluation, J. Hazard. Mater. 320 (2016) 296–303.

[20] Q. Sun, G. Zhu, J. Wu, J. Lu, Z. Zhang, Catalytic ozonation of nitroimidazole antibiotics using nano-magnesium hydroxide as heavy-metals free catalyst, Desalin. Water Treat. 161 (2019) 216–227.

[21] M. Shao, F. Ning, J. Zhao, M. Wei, D.G. Evans, X. Duan, Preparation of Fe$_3$O$_4$@SiO$_2$@Layered double hydroxide core-shell microspheres for magnetic separation of proteins, J. Am. Chem. Soc. 134 (2012) 1071–1077.

[22] H. Liu, P. Zeng, S. Ji, J. Ji, W. Yang, Y. Li, Synthesis of TiO$_2$/SiO$_2$@Fe$_3$O$_4$ magnetic microspheres and their properties of photocatalytic degradation dyestuff, Catal. Today 175 (2011) 293–298.

[23] Z.-Q. Liu, J. Ma, Y.-H. Cui, L. Zhao, B.-P. Zhang, Influence of different heat treatments on the surface properties and catalytic performance of carbon nanotube in ozonation, Appl. Catal. B-Environ. 101 (2010) 74–80.

[24] H. Hu, Z. Wang, L. Pan, S. Zhao, S. Zhu, Ag-coated Fe$_3$O$_4$@SiO$_2$ three-ply composite microspheres: synthesis, characterization, and application in detecting melamine with their surface-enhanced Raman scattering, J. Phys. Chem. C. 114 (2010) 7738–7742.

[25] A. Mashayekh-Salehi, G. Moussavi, K. Yaghmaeian, Preparation, characterization and catalytic activity of a novel mesoporous nanocrystalline MgO nanoparticle for ozonation of acetaminophen as an emerging water contaminant, Chem. Eng. J. 310 (2017) 157–169.

[26] R. Yin, W. Guo, X. Zhou, H. Zheng, J. Du, Q. Wu, J. Chang, N. Ren, Enhanced sulfamethoxazole ozonation by noble metal-free catalysis based on magnetic Fe$_3$O$_4$ nanoparticles: catalytic performance and degradation mechanism, Rsc. Adv. 6 (2016) 19265–19270.

[27] G. Moussavi, A. Khavanin, R. Alizadeh, The integration of ozonation catalyzed with MgO nanocrystals and the biodegradation for the removal of phenol from saline wastewater, Appl. Catal. B-Environ. 97 (2010) 160–167.

[28] B. Lan, R. Huang, L. Li, H. Yan, G. Liao, X. Wang, Q. Zhang, Catalytic ozonation of p-chlorobenzoic acid in aqueous solution using Fe-MCM-41 as catalyst, Chem. Eng. J. 219 (2013) 346–354.

[29] Y. Li, X. Zhao, Y. Yan, J. Yan, Y. Pan, Y. Zhang, B. Lai, Enhanced sulfamethoxazole degradation by peroxymonosulfate activation with sulfide-modified microscale zero-valent iron (S-mFe0): Performance, mechanisms, and the role of sulfur species, Chem. Eng. J. 376 (2019) 121302.